Proceedings of the 7th International Conference on Civil Structural and Transportation Engineering (ICCSTE'22)
Niagara Falls, Canada – June 05-07, 2022
Paper No. 221
DOI: 10.11159/iccste22.221

Numerical Analysis Of Circular Concrete-Filled Stainless Steel Tubular Short Columns Under Axial Loading

Mizan Ahmed[1], Soheil Gohari[2], Khaled Sennah[3], Wensu Chen[1]
[1] School of Civil and Mechanical Engineering, Curtin University, Kent Street, Bentley, WA 6102, Australia
[2]Department of Mechanical Engineering, The University of Melbourne, Parkville, VIC 3010, Australia
[3] Department of Civil Engineering, Ryerson University, Toronto, Canada
mizan.ahmed@curtin.edu.au; soheil.gohari@unimelb.edu.au; ksennah@ryerson.ca; wensu.chen@curtin.edu.au

Abstract **–** This paper develops a simplified fiber-based numerical model to investigate the performance of circular concrete-filled stainless steel tubular (CFSST) short columns subjected to axial loading. A new compressive concrete strength formula is developed based on the test data of CFSST columns. The accuracy of the numerical model is evaluated by comparing the ultimate axial capacity and axial load–strain curves of CFSST columns with a large test database. A parametric study is carried out to investigate the effects of geometry and material properties on the axial performance of CFSST columns.

Keywords**:** *Concrete-filled steel tubes; axial loading; short columns; nonlinear analysis.*

1. Introduction

The composite action between the steel and concrete of concrete-filled steel tubular (CFST) columns results in improved structural performance in terms of strength, ductility, fire and seismic resistance compared to that of reinforced concrete columns. The lateral confinement inserted by steel tube to the confined concrete is more effective in circular CFST columns compared to its rectangular and square counterparts, thus widely used in the construction of high-rise buildings and bridge piers to carry large axial loads [1]. However, the steel tube of CFST columns may be subjected to corrosion which may reduce their axial performance. As stainless steel offers excellent corrosion resistance, circular concrete-filled stainless steel tubular (CFSST) columns were proposed. Owing to the distinguished strain hardening behavior of stainless steel, the performance of CFSST columns is different than that of CFST columns with carbon steel. In addition, the cost-effective design of CFSST columns is important considering the higher cost of stainless steel than carbon steel. However, there is a lack of research in the development of an accurate numerical model to study their axial performance.

Test on circular CFSST short columns subjected to axial loading was carried out by [2-14]. The test results showed that CFSST columns have higher ultimate strength and ductility compared to that CFST columns. The experimental program reported in the literature examined the influences of a wide range of column parameters of CFSST columns under axial loading including the tube diameter [2-4, 6-8, 10, 12, 15], tube thickness [4, 6, 8, 12, 14], concrete strength [2-4, 6, 7, 11, 14], recycled aggregates [5, 9], and column slenderness ratio [3, 10-12]. The axial behavior of CFSST columns was numerically investigated by [13], [15], [16], [17] and [18]. Patel et al. [16] concluded that the conventional lateral pressure model for carbon steel underestimated the axial performance of CFSST columns. However, until today no effort was made to develop a lateral pressure model for CFSST columns.

This paper develops a numerical model using a fiber model to investigate the axial performance of CFSST short columns under axial loading. An accurate formula to predict the compressive strength of concrete of CFSST columns is developed based on the existing experimental data. The accuracy of the numerical prediction is validated using a large test database comprising of test data of 125 short columns. A parameter study is carried out to study the influences of geometry and material properties of CFSST columns on their axial performance.

2. Numerical Model

The numerical model is developed using the fiber analysis theory, where the cross-section of the CFSST column is divided into small fibers, as shown in Fig. 1. The fibers either represent the properties of stainless steel or concrete based on the uniaxial material laws assigned to them. The computational analysis starts with initializing a small axial strain and then calculating the stresses occurring in fibers using the uniaxial material laws assigned to them. The column axial load (P) is calculated as the resultant stress. The theoretical analysis continues for the increase of the axial strain until the maximum column axial load (P_{ult}) is achieved. The stopping criterion is chosen when P drops to $0.5P_{ult}$ or the axial strain exceed the prescribed ultimate strain of concrete ($\varepsilon \geq \varepsilon_{cu}$). The analysis steps to predict the full axial load-strain ($P-\varepsilon$) curves of CFSST columns are given as follows:

(1) Input details of CFSST column.
(2) Divide the cross-section into fine fibers.
(3) Initialize strain as $\varepsilon = \Delta\varepsilon$.
(4) Calculate fiber stresses using the material uniaxial stress-strain relationships.
(5) Compute the axial force P as the stress resultant.
(6) Increase axial strain by $\varepsilon = \varepsilon + \Delta\varepsilon$.
(7) Repeat Steps 4 to 6 until $P \leq 0.5P_{ult}$ or $\varepsilon \geq \varepsilon_{cu}$.
(8) Plot $P-\varepsilon$ curve.

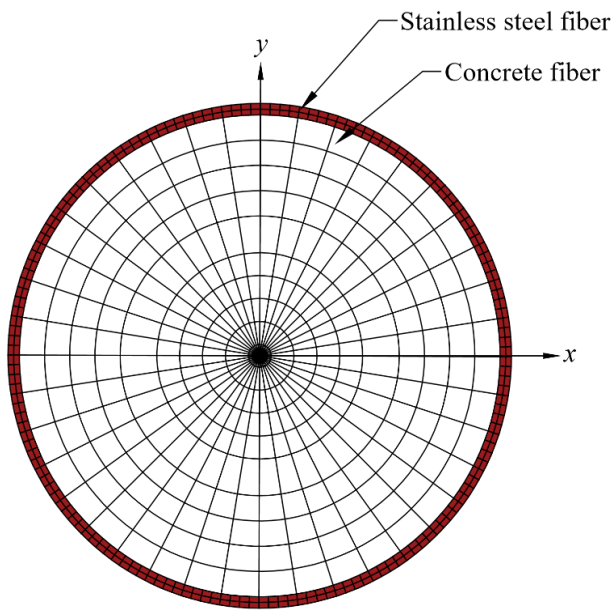

Fig. 1: Discretization of the cross-section of a CFSST column in fiber analysis method.

3. Material properties

3.1 Stainless steel

The stress-strain relationships of stainless steel proposed by Quach et al. [19] are adopted in this study. The original formulae proposed by Quach et al. [19] to calculate the full stress-strain curves of stainless steel is stress-dependent. Abdella et al. [20] suggested formulae to derive the inverse version of the stress-strain relationships of stainless steel proposed by Quach et al. [19] to calculate the full ranges of the tensile and compressive stresses of stainless steel in the function of strain. The three-stage stress-strain relationships of stainless steel developed by Quach et al. [19] provide a better estimation than the existing two-stage constitutive laws of stainless steel [16, 21].

3.2 Concrete

Figure 2 illustrates the stress-strain relationships of concrete adopted in this study [22]. The axial stress of concrete (σ_c) at the ascending branch of the curve is calculated using the formulae developed by Mander et al. [23]:

$$\sigma_c = \frac{f_{cc}^{'}(\varepsilon_c / \varepsilon_{cc}^{'})\lambda}{(\varepsilon_c / \varepsilon_{cc}^{'})^{\lambda} + \lambda - 1} \qquad \text{for} \quad 0 \le \varepsilon_c \le \varepsilon_{cc}^{'} \tag{1}$$

$$\lambda = \frac{E_c \varepsilon_{cc}^{'}}{E_c \varepsilon_{cc}^{'} - f_{cc}^{'}} \tag{2}$$

where, ε_c is the concrete strain; $f_{cc}^{'}$ and $\varepsilon_{cc}^{'}$ are the concrete compressive strength and the corresponding strain, respectively; E_c is the elastic modulus of concrete, calculated as [22]:

$$E_c = 4400\sqrt{\gamma_c f_c^{'}} \tag{3}$$

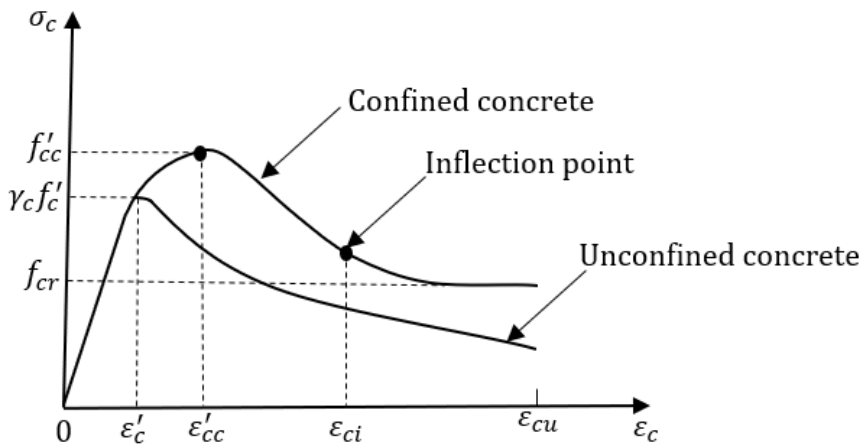

Fig. 2. Stress-strain relationship of concrete [22].

The column size on the compressive strength of unconfined concrete ($f_c^{'}$) is considered using a reduction factor (γ_c), developed by Liang [24] as $\gamma_c = 1.85 D_c^{-0.135}$, where, $D_c = D - 2t$, in which D and t are the diameter and thickness of the steel tube, respectively.

As discussed earlier, the lateral confinement provided by the steel tube improves the strength and ductility of the confined concrete which is considered in the stress-strain relationships of concrete. A new formula to calculate the compressive strength of concrete ($f_{cc}^{'}$) of CFSST columns is developed by analyzing the existing test data of CFSST columns. Parameter study demonstrates that $f_{cc}^{'}$ is influenced by the confinement factor (ξ), which can be calculated as $\xi = A_s \sigma_{0.2} / A_c \gamma_c f_c^{'}$, where, $\sigma_{0.2}$ is the yield stress of stainless steel taken as 0.2% proof stress; $f_c^{'}$ is the compressive strength of unconfined concrete; A_s and A_c are the area of steel and concrete, respectively. The test compressive strength of confined concrete ($f_{cc,test}^{'}$) of tested columns is determined by subtracting the axial capacity of the stainless steel tube from the ultimate axial load of CFSST columns. Based on the regression analysis, a formula to calculate the compressive strength of confined concrete is proposed herein as:

$$\frac{f_{cc}^{'}}{f_c^{'}} = 0.44\xi + 0.9 \ge 1.0 \tag{4}$$

Wang et al. [25] suggested a formula to calculate the compressive strain of confined concrete $\left(\varepsilon_{cc}^{'}\right)$:

$$\varepsilon_{cc}^{'} = 3000 - 10.4\left(\sigma_{0.2}\right)^{1.4}\left(f_c^{'}\right)^{-1.2}\left[0.73 - 3785.8\left(\frac{D}{t}\right)^{-1.5}\right] \le 0.01 \tag{5}$$

The axial stress of concrete at the descending branch of the stress-strain curves is calculated using the formula developed by Lim and Ozbakkaloglu [22] as:

$$\sigma_c = f_{cc}^{'} - \frac{f_{cc}^{'} - f_{cr}}{1 + \left(\frac{\varepsilon_c - \varepsilon_{cc}^{'}}{\varepsilon_{ci} - \varepsilon_{cc}^{'}}\right)^{-2}} \qquad \text{for} \quad \varepsilon_c > \varepsilon_{cc}^{'} \tag{6}$$

where, f_{cr} is the residual strength of concrete, calculated as $f_{cr} = \beta_c f_{cc}^{'}$, where, β_c is the strength degradation parameter developed by Ahmed et al. [26] as:

$$\beta_c = 1.2420 - 0.0029\left(\frac{D}{t}\right) - 0.0044\, f_c^{'} \quad \text{where} \ \left(0 < \beta_c \le 1.0\right) \tag{7}$$

The strain at the inflection point (ε_{ci}) is calculated as [22]:

$$\varepsilon_{ci} = 2.8\varepsilon_{cc}^{'}\left(f_c^{'}\right)^{-0.12}\left(\frac{f_{cr}}{f_{cc}^{'}}\right) + 10\varepsilon_{cc}^{'}\left(f_c^{'}\right)^{-0.47}\left(1 - \frac{f_{cr}}{f_{cc}^{'}}\right) \tag{8}$$

4. Validation

The numerical model is validated by comparing the predicted ultimate load and $P-\varepsilon$ curves of CFSST columns with the ones obtained from the test study. A total of 125 test data is used for validation purposes. The comparison between the test and predicted ultimate load of CFSST columns is shown in Fig. 3, where it can be seen that the numerical model can provide a reasonable estimation of the ultimate strength of CFSST short columns subjected to axial loading. From Fig. 4, it also can be seen that the numerical model can accurately predict the $P-\varepsilon$ curves of CFSST columns.

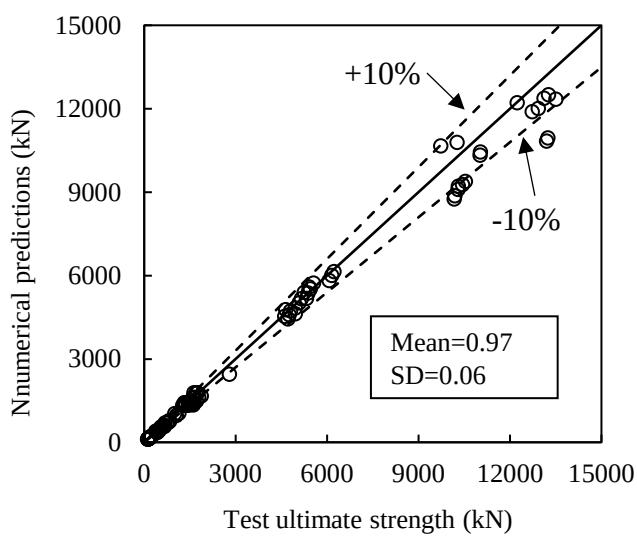

Fig. 3. Comparison of the predicted ultimate strength of CFSST columns with the experimental results.

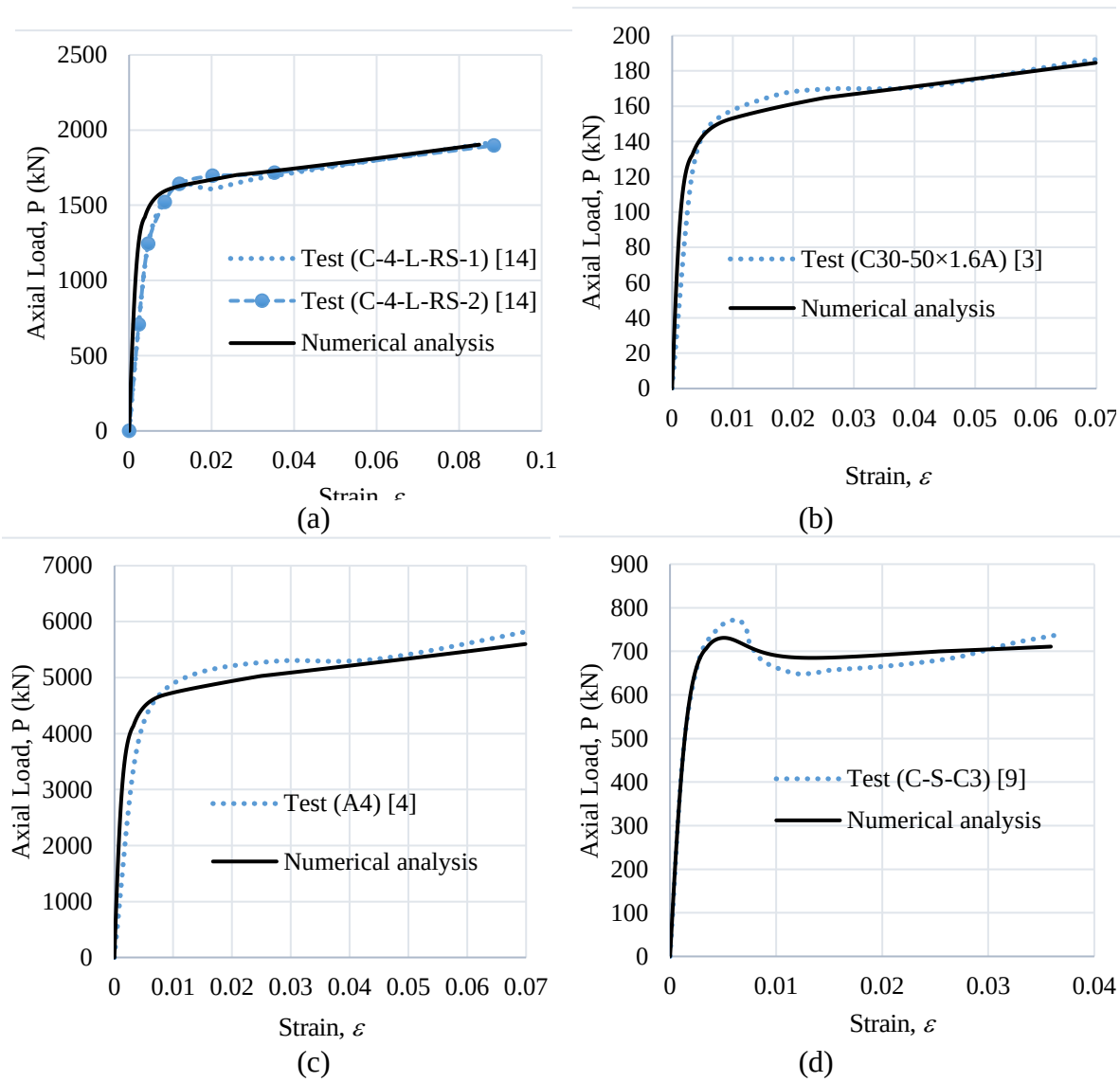

Fig. 4. Comparison of the predicted $P-\varepsilon$ curves of CFSST columns with the experimental results.

5. Parametric study

The validated numerical model is used to carry out a parameter study to investigate the effects of diameter-to-thickness (D/t) ratio, concrete compressive strength and the yield stress of steel on the axial performance of CFSST columns. The details of the reference column are as follows: $D=500$ mm; $t=10$ mm, $f_c^{'}=50$ MPa, $\sigma_{0.2}=205$ MPa.

5.1 Effects of the diameter-to-thickness (D/t) ratio

The D/t ratio of the CFSST column is an important column parameter that influences their axial performance. In this study, the thickness of the steel tubes is changed to vary the D/t ratio from 25 to 100. As illustrated in Fig. 5, it was found that increasing the D/t ratio from 25 to 100 decreases the ultimate load of CFSST columns by 51.4%. This is because decreasing the thickness of the steel tube wall reduces the confinement effect. The ductility of the CFSST column is also decreased as the D/t ratio increases, as can be seen in Fig. 5.

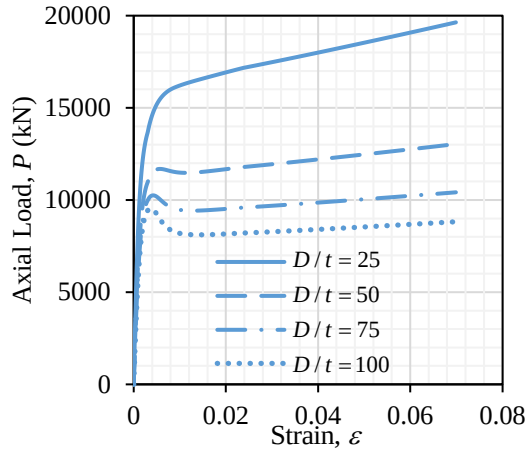

Fig. 5. Influences of D/t ratio on the $P-\varepsilon$ curves.

5.2 Effects of concrete compressive strength

The influences of concrete strength on the axial performance of the CFSST column are investigated by changing the concrete strength from 25 MPa to 100 MPa. It is seen from Fig. 6 that increasing concrete strength increases the axial capacity of the columns. When concrete strength increases from 25 MPa to 100 MPa, the ultimate load is increased by 79.2%. However, increasing concrete strength decreases the ductility of the columns. This is due to the brittle nature of high-strength concrete.

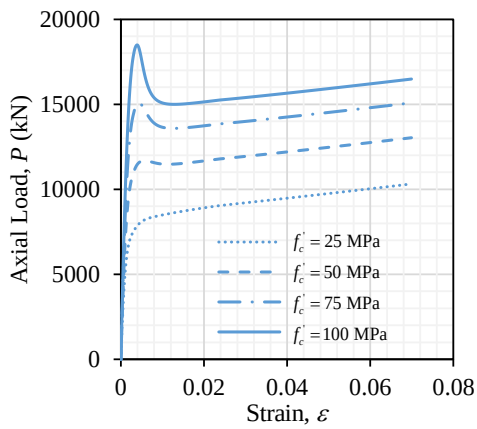

Fig. 6. Influences of concrete compressive strength on the $P-\varepsilon$ curves.

5.3 Effects of steel yield stress

To study the effects of steel yield stress, the axial performance of the CFSST column is investigated for different grades of stainless steel, namely austenitic, ferritic and duplex stainless steel. The yield stress of the austenitic, ferritic and duplex stainless steel are taken as 205, 275 and 430 MPa, respectively based on suggestions given in AS/NZS 4673-2001 [27]. It is found that with a steel yield stress increased from 205 MPa to 430 MPa, the ultimate load of the CFSST column is increased by 48.1%, as illustrated in Fig. 7. However, the steel yield stress has insignificant effects on the ductility of the CFSST column.

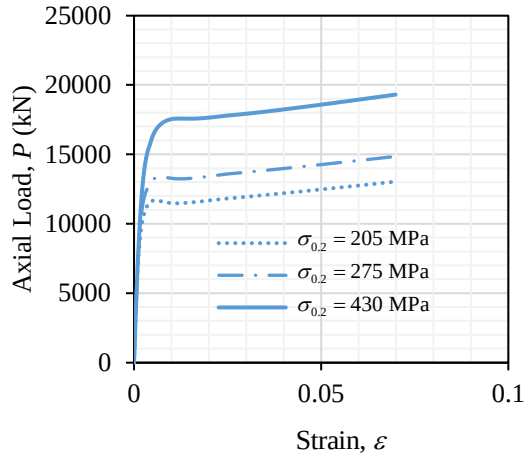

Fig. 7. Influences of steel yield stress on the $P-\varepsilon$ curves.

6. Conclusion

This paper develops a numerical model to study the performance of CFSST columns under axial loading. A new formula to calculate the compressive strength of concrete is developed based on the existing test data. Upon validation, the numerical model is used to perform a parametric study to study the effects of the D/t ratio, the yield stress of steel and concrete strength on their axial performance. It is found that the numerical model can accurately predict the axial performance of the CFSST column observed experimentally. The parametric study shows that increasing D/t ratio reduces the ultimate load of CFSST columns whereas increasing the yield stress of steel or concrete strength increases their ultimate load. However, the ductility of the CFSST column is reduced as the D/t ratio or the concrete strength increases.

References

[1] Ahmed M, Liang QQ, Patel VI, and Hadi MNS. Nonlinear analysis of rectangular concrete-filled double steel tubular short columns incorporating local buckling. Engineering Structures 2018;175:13-26.

[2] Lam D and Gardner L. Structural design of stainless steel concrete filled columns. Journal of Constructional Steel Research 2008;64(11):1275-1282.

[3] Uy B, Tao Z, and Han LH. Behaviour of short and slender concrete-filled stainless steel tubular columns. Journal of Constructional Steel Research 2011;67(3):360-378.

[4] Peng D, Lu Y, Xuan W, and Yu-hang Z. Experimental studies on the behavior and capacity of concrete filled stainless steel tube short columns. Engineering Mechanics 2019;36(S1):298-305.

[5] Tam VW, Wang Z-B, and Tao Z. Behaviour of recycled aggregate concrete filled stainless steel stub columns. Materials and structures 2014;47(1):293-310.

[6] Dai P, Yang L, Wang J, and Zhou Y. Compressive strength of concrete-filled stainless steel tube stub columns. Engineering Structures 2020;205:110106.

[7] Li Y, Zhao X, Singh RR, and Al-Saadi S. Tests on seawater and sea sand concrete-filled CFRP, BFRP and stainless steel tubular stub columns. Thin-Walled Structures 2016;108:163-184.

[8] Li Y, Zhao X, Raman RS, and Yu X. Axial compression tests on seawater and sea sand concrete-filled double-skin stainless steel circular tubes. Engineering Structures 2018;176:426-438.

[9] Yang Y-F and Ma G-L. Experimental behaviour of recycled aggregate concrete filled stainless steel tube stub columns and beams. Thin-Walled Structures 2013;66:62-75.

[10] Li D, Uy B, Aslani F, and Hou C. Behaviour and design of spiral-welded stainless steel tubes subjected to axial compression. Journal of Constructional Steel Research 2019;154:67-83.

[11] Ellobody E and Ghazy MF. Experimental investigation of eccentrically loaded fibre reinforced concrete-filled stainless steel tubular columns. Journal of constructional steel research 2012;76:167-176.

[12] Chen Y, Li F, and Wang J. Experimental study on axial compressive behavior of concrete-filled thermoforming stainless steel tubular stub columns. Journal of Building Structures 2013;34(2):106-112.

[13] He A, Su A, Liang Y, and Zhao O. Experimental and numerical investigations of circular recycled aggregate concrete-filled stainless steel tube columns. Journal of Constructional Steel Research 2021;179:106566.
[14] Liao F-Y, Hou C, Zhang W-J, and Ren J. Experimental investigation on sea sand concrete-filled stainless steel tubular stub columns. Journal of Constructional Steel Research 2019;155:46-61.
[15] He A and Zhao O. Experimental and numerical investigations of concrete-filled stainless steel tube stub columns under axial partial compression. Journal of Constructional Steel Research 2019;158:405-416.
[16] Patel VI, Liang QQ, and Hadi MNS. Nonlinear analysis of axially loaded circular concrete-filled stainless steel tubular short columns. Journal of Constructional Steel Research 2014;101:9-18.
[17] Li Y, Zhao X, and Raman RS. Theoretical model for concrete-filled stainless steel circular stub columns under axial compression. Journal of Constructional Steel Research 2019;157:426-439.
[18] Ding F-x, Yin Y-x, Mao J-f, Wang L-p, Yu Y-j, Luo L, and Yu Z-w, "Analytical behaviors of concrete-filled circular stainless steel tubular (CFCSST) stub columns under axial loading," in *Structures*, 2019, vol. 19, pp. 277-285.
[19] Quach W, Teng JG, and Chung K. Three-stage full-range stress-strain model for stainless steels. Journal of Structural Engineering 2008;134(9):1518-1527.
[20] Abdella K, Thannon RA, Mehri AI, and Alshaikh FA. Inversion of three-stage stress–strain relation for stainless steel in tension and compression. Journal of Constructional Steel Research 2011;67(5):826-832.
[21] Tao Z, Uy B, Liao FY, and Han LH. Nonlinear analysis of concrete-filled square stainless steel stub columns under axial compression. Journal of Constructional Steel Research 2011;67(11):1719-1732.
[22] Lim JC and Ozbakkaloglu T. Stress–strain model for normal-and light-weight concretes under uniaxial and triaxial compression. Construction and Building Materials 2014;71:492-509.
[23] Mander JB, Priestley MJN, and Park R. Theoretical stress-strain model for confined concrete. Journal of Structural Engineering 1988;114(8):1804-1826.
[24] Liang QQ. Nonlinear analysis of circular double-skin concrete-filled steel tubular columns under axial compression. Engineering Structures 2017;131:639-650.
[25] Wang Z, Tao Z, Han LH, Uy B, Lam D, and Kang WH. Strength, stiffness and ductility of concrete-filled steel columns under axial compression. Engineering Structures 2017;135:209-221.
[26] Ahmed M, Liang QQ, Patel VI, and Hadi MNS. Numerical analysis of axially loaded circular high strength concrete-filled double steel tubular short columns. Thin-Walled Structures 2019;138:105-116.
[27] AS/NZS 4673-2001. Cold-formed Stainless Steel Structures. Australian/New Zealand Standard, Sydney, NSW, Australia. 2001.